JOURNAL OF MATERIALS SCIENCE **39** (2004) 779–785

# Electrophoretic deposition for coatings and free standing objects

O. VAN DER BIEST, S. PUT, G. ANNÉ, J. VLEUGELS
*Department of Metallurgy and Materials Engineering, Katholieke Universiteit Leuven, Kasteelpark Arenberg 44, B-3001 Leuven, Belgium*
*E-mail: omer.VanderBiest@mtm.kuleuven.ac.be*

A simulation of the electrophoretic deposition process is presented, which allows one to predict the yield of deposition as a function of time for different values of the electrical properties of the liquid and the powders used. It is shown that with special precautions, conditions can be defined where the resistance of the deposit will limit its thickness. Under most conditions however, particularly if a liquid with reasonable electrical conductivity is used, the resistance of the deposit should not limit its growth. Other issues which are of importance in the shaping of free standing objects are also discussed, in particular the electrode shape and electric field distribution, separation of the deposit from the electrode and drying of the object. 

## 1. Introduction

Electrophoretic deposition (EPD) for shaping of materials can be applied to any solid that is available in the form of a fine powder (<30 $\mu$m) including metals, polymers and glasses [1]. Furthermore, the process can be used for producing coatings as well as free standing objects. It is the purpose of this contribution to highlight some of the characteristics of the process so as to come to a view on why one would want to use it in preference to other processes which are available for applying coatings or to form components from powders. We will limit ourselves to the use of non-aqueous suspensions, even though EPD from aqueous suspensions is possible [2].

First a process simulation model for plate-shaped components is presented that predicts conditions for which the electric field across the deposit plays an important role so that it can limit further deposition. The model shows that under most conditions the deposition can continue for a very large thickness. In a second part, we will describe some limitations in the shaping capability of EPD due to complex electric field distributions and review some of the additional issues that need to be resolved for a successful EPD process. Electric field calculations are carried out by using commercially available software. The linkage between parts 1 and 2 is thus the important role of the electric field during EPD of plate-shaped as well as more complex shaped components.

## 2. Modeling of the EPD process

### 2.1. Description

The empirical equation of Hamaker [3] gives the relation between the instantaneous yield rate and the electric field.

$$\frac{\mathrm{d}Y}{\mathrm{d}t} = f\mu ECA \tag{1}$$

with the yield $Y$ (kg), time $t$ (s), the electrophoretic mobility $\mu$ ($m^2/V \cdot s$), the electric field strength $E$ (V/m), the solids loading $C$ ($kg/m^3$) of the powder in suspension and the surface area $A$ ($m^2$) of the electrode; $f$ is a factor that takes into account that not all powder brought to the electrode may be incorporated in the deposit. In this work $f$ is assumed to be 1. The electric field may play an important role during deposition of plate-shaped as well as complex geometries. In the following, the role of the electric field strength will be discussed for planar geometries. For this purpose a model is developed based on Hamaker's Equation 1. Paragraph 3 will focus on the EPD of more complex geometries.

Sussman and Ward [4] developed a model to predict the kinetics of deposition. They assumed a constant particle concentration in suspension, which in general is not valid. Moreover, although they mentioned that the charge carriers present in suspension represent the sum of ions in the liquid and charges associated with the powder particles, they did not incorporate both charge carriers in their model. Based on Faraday's law, Hirata *et al.* [5] developed a model to predict the deposited mass as a function of deposition time. However, they did not take into account the influence of the deposit resistance as well as the influence of different charge carriers, being the powder particles as well as ionic contributions in the liquid solvent, on the deposition kinetics. Therefore in the following, a model is presented, which incorporates both ion and particles as charge carriers in suspension as well as in the formed deposit. Also the

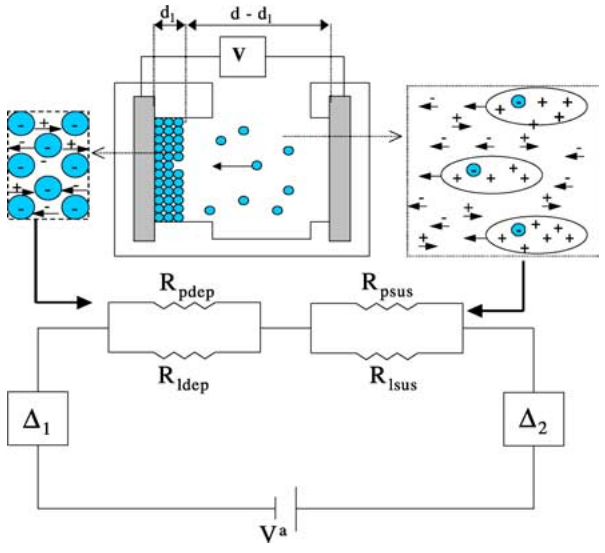


*Figure 1* The currents and voltages during the EPD process are calculated from the equivalent electric circuit shown.

changing powder concentration in suspension during the EPD process is taken into account.

The electric field at a planar deposit can be calculated from an equivalent electric circuit as shown in Fig. 1, in which four resistances appear: two to describe conduction in the suspension and two for the deposit. In the suspension, current is carried by individual ions dissolved in the liquid and by the powder with its associated ion cloud, as mentioned in [4]. Hence for the suspension the resistances are:

$$R_{\text{lsus}} = \frac{(d - d_{\text{l}})}{\sigma_{\text{lsus}} A} \tag{2}$$

$$R_{\text{psus}} = \frac{(d - d_{\text{l}})}{\mu \cdot A \cdot C \cdot Q_{\text{eff}}} \tag{3}$$

where $R_{\text{lsus}}$ represents the resistance of the ions in the liquid, $R_{\text{psus}}$ the resistance of the powder particles in suspension, $d$ is the electrode distance (m); $d_{\text{l}}$ the deposit thickness (m); $Q_{\text{eff}}$ the effective powder charge (C/kg); $\sigma_{\text{lsus}}$ is the specific conductivity of the liquid in suspension (S/m).

The deposit is assumed to be made-up of a powder bed with resistance $R_{\text{pdep}}$ with a packing fraction '$p$' and an interparticle liquid phase with total resistance $R_{\text{ldep}}$. The corresponding resistances are:

$$R_{\text{pdep}} = \frac{d_{\text{l}}}{\sigma_{\text{pdep}} \cdot p \cdot A} \tag{4}$$

$$R_{\text{ldep}} = \frac{d_{\text{l}}}{\sigma_{\text{ldep}}(1 - p) \cdot A} \tag{5}$$

where $\sigma_{\text{pdep}}$ is the specific conductivity of the (dry) powder in the deposit (S/m), which we have derived from the resistivity of bulk material. The conductivity in the interparticle liquid in the deposit, $\sigma_{\text{ldep}}$, is related to that in the suspension, $\sigma_{\text{lsus}}$, but it is likely to be higher due to the fact that the particles release their cloud of counter-ions at the electrode, thus $\sigma_{\text{ldep}} = \lambda \cdot \sigma_{\text{lsus}}$ with $\lambda \geq 1$.

Using the equivalent electrical scheme of Fig. 1, the total resistance of the deposition cell can be calculated as:

$$R_{\text{tot}} = \left[\frac{1}{R_{\text{psus}}} + \frac{1}{R_{\text{lsus}}}\right]^{-1} + \left[\frac{1}{R_{\text{pdep}}} + \frac{1}{R_{\text{ldep}}}\right]^{-1} = \frac{R_{\text{psus}} R_{\text{lsus}}}{R_{\text{psus}} + R_{\text{lsus}}} + \frac{R_{\text{pdep}} R_{\text{ldep}}}{R_{\text{pdep}} + R_{\text{ldep}}} \tag{6}$$

If the potential drop at the electrodes due to polarization, $\Delta V_{\text{i}}^{\text{e}}$, is neglected the total current $I$ flowing through the deposition cell can be calculated from Ohm's law as:

$$I = \frac{V^{\text{a}}}{R_{\text{tot}}} = \frac{V^{\text{a}}}{\frac{d - d_{\text{l}}}{\mu A c Q_{\text{eff}} + \sigma_{\text{lsus}} A} + \frac{d_{\text{l}}}{\sigma_{\text{pdep}} A p + \lambda \sigma_{\text{lsus}} A (1-p)}} \tag{7}$$

With $V^{\text{a}}$, the applied voltage ($V$). The voltage drop difference between the deposition front and the counter electrode, $\Delta V^{\text{sus}}$ divided by the distance between them gives an expression for the electric field strength at the deposition plane:

$$E = \frac{\Delta V^{\text{sus}}}{(d - d_{\text{l}})} = \frac{V^{\text{a}} - I \frac{R_{\text{pdep}} R_{\text{ldep}}}{R_{\text{pdep}} + R_{\text{ldep}}}}{d - d_{\text{l}}} \tag{8}$$

An expression for the yield of deposition as function of time can be obtained by substituting Equations 2 till (8) in (1), which becomes:

(a) for a constant powder loading $C$ during EPD:

$$\mathrm{d}Y = f \mu A^2 V^{\text{a}} C \rho_{\text{dep}} \times \frac{(\sigma_{\text{pdep}} A p + \lambda \sigma_{\text{lsus}} A (1 - p))}{(\sigma_{\text{pdep}} A p + \lambda \sigma_{\text{lsus}} A (1 - p))(\rho_{\text{dep}} A d - Y) + Y(\mu A c Q_{\text{eff}} + \sigma_{\text{lsus}} A)} \mathrm{d}t \tag{9a}$$

(b) for a decreasing powder loading $C = \frac{M_0 - Y}{v}$ during EPD:

$$\mathrm{d}Y = \frac{f \mu A^2 V^{\text{a}} \rho_{\text{dep}}}{v} \times \frac{(\sigma_{\text{pdep}} A p + \lambda \sigma_{\text{lsus}} A (1 - p))(M_0 - Y)}{(\sigma_{\text{pdep}} A p + \lambda \sigma_{\text{lsus}} A (1 - p))(\rho_{\text{dep}} A d - Y) + Y(\mu A c Q_{\text{eff}} + \sigma_{\text{lsus}} A)} \mathrm{d}t \tag{9b}$$

with $M_0$, the initial mass of powder in suspension (kg), $\rho_{\text{dep}}$, the theoretical density of the powder (kg/m$^3$) and $v$, the volume of suspension (m$^3$).

Using this model, one can derive the yield as function of time for different values of the different resistances involved. Voltage drops due to polarization processes at the electrodes are neglected in our simulations. Such effects are minimized if the suspension is circulating or stirred during deposition.

It is commonly believed that the electrical resistance of the deposit may reduce the yield and eventually stop the EPD process [4]. Fig. 2 shows the total yield predicted by the equations above as well as experimentally determined for a value of the electrical conductivity of the polar liquids which we use commonly in our work on free standing objects. Table I gives more details about the parameters incorporated in the model to predict the yield of alumina powder deposited as

TABLE I Parameters used in the model during EPD of alumina from a suspension of acetone with 10 vol% *n*-butylamine

| | Parameters |
|---|---|
| Applied voltage $V^a$ (V) | 300 |
| Deposition time, $t$ (s) | 300 |
| Electrophoretic mobility, $\mu$ ($m^2/V{\cdot}s$) | $12.4 \times 10^{-5}$ |
| Packing factor, $p$ | 0.45 |
| Electrode surface, $A$ ($cm^2$) | 9 |
| Electrode distance, $d$ (cm) | 3.5 |
| Initial solids loading, $M_0$ (g) | 5 |
| Volume of suspension, $v$ ($cm^3$) | 50 |
| Theoretical density $Al_2O_3$, $\rho_{dep}$ ($g/cm^3$) | 3.89 |
| Effective powder charge, $Q_{eff}$(mC/g) | 53 |
| Specific conductivity ions in suspension, $\sigma_{lsus}$($\mu$S/cm) | 2.85 |
| Ionic factor, $k$ | 2 |

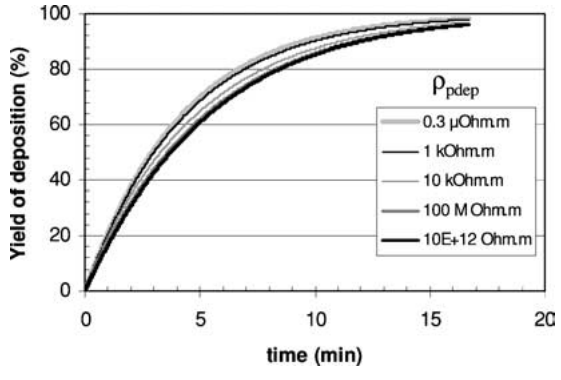


*Figure 2* Yield as a percentage of the total available powder in the suspension. The specific conductivity of the suspension liquid $\sigma_{lsus}$ is assumed to be constant at 2 $\mu$S/cm, which corresponds to the experimental results of Fig. 3. Different curves show the effect of a changing specific resistivity for the dry powder $\rho_{pdep}$ from a good conductor to a good insulator.

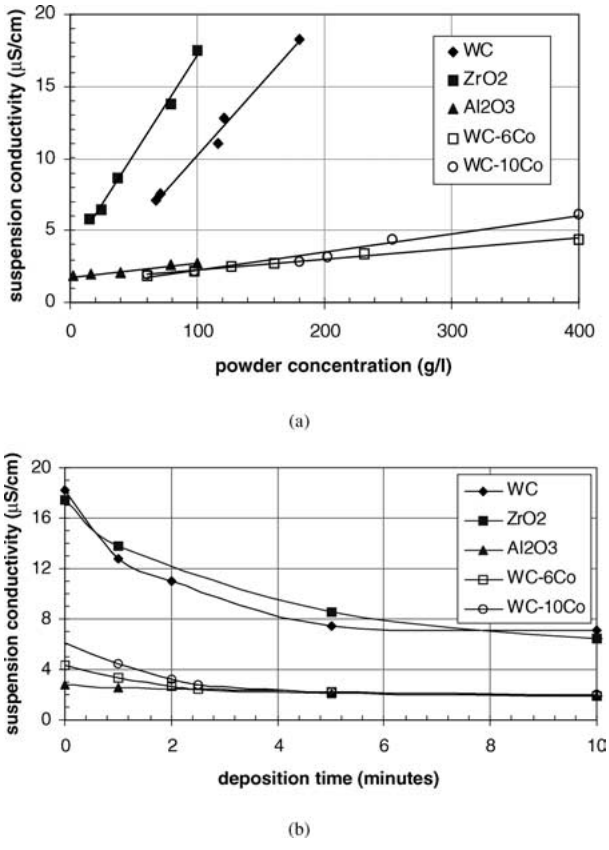


*Figure 3* Suspension conductivity as a function of (a) remaining powder concentration in suspension during EPD and (b) deposition time for different powders in acetone/*n*-butylamine.

function of time in an acetone/*n*-butylamine suspension (10 vol%). More details about these parameters can be found in [6].

The conclusion is that in general thick deposits can be created by EPD of the order of several cm even for powders which in dry condition are excellent insulators. As shown in Fig. 2 the thickness of a deposit can always be controlled by the total supply of powder available in the suspension.

## 2.2. Influence of the resistivity of the liquid

The total suspension conductivity may remain essentially constant or may evolve with time as deposition proceeds. The suspension conductivity, $S_{sus}$, during electrophoretic deposition is proportional with the concentration of charge carriers in suspension, i.e., powder particles, as expressed by Equation 3 and ionic species present in the liquid of the suspension, as expressed by Equation 2. We will use experimental measurements of conductivity of different powders, which we have deposited over the years from an acetone/*n*-butylamine medium. These experimental results show that the conductivity during EPD decreases linearly with decreasing powder concentration (Fig. 3a). For these experiments in acetone/*n*-butylamine, $S_{sus}$ can be described as:

$$S_{sus} = aC + b \tag{10}$$

with $C$, the powder concentration in suspension; $a$, the slope and $b$, the intercept. If a suspension is used, with an initial mass of powder $M_0$ and a volume, $v$, the powder concentration $C$ decreases during EPD with increasing yield of deposition, $Y$ as:

$$C = \frac{M_0 - Y}{v} \tag{11}$$

Incorporation of Equation 11 in Hamaker's equation, with the assumption of a constant electric field as would be the case if the powder itself is a good conductor, shows that the deposition yield decreases in an exponential way during electrophoretic deposition from an acetone/*n*-butylamine suspension:

$$Y = M_0\left[1 - e^{-\frac{\mu EA}{v}t}\right] \tag{12}$$

By incorporating Equations 11 and 12 in 10, $S_{sus}$ can be expressed as a function of time as:

$$S_{sus} = a\frac{M_0}{V_0}e^{-\frac{\mu EA}{V_0}t} + b \tag{13}$$

Hence from the reduction of particle concentration alone an exponential decrease with time of the total suspension conductivity is predicted, superimposed on

a background in conductivity due to the ionic species. It is possible that the decrease in suspension conductivity is not only caused by a decreasing concentration of powder particles, but that also the concentration of ionic species evolves with time due to homogeneous chemical reactions in the suspension or electrochemical reactions at the electrodes. Such reactions are system specific and there is in fact not a lot of information available for most solvents apart from the common case of water. Nevertheless, these reactions may also give rise to changes in conductivity which are not linear with time and an exponential decrease is also possible e.g., due to reduction of ions at the cathode.

In order to continue our modeling efforts in which we would like to cover a wide range of conditions, we have modeled EPD behavior for a range of behaviors of the conductivity (or resistivity) in the suspension liquid as a function of time, as shown in Fig. 4a. This includes an exponential increase in resistivity of the suspension liquid as a function of time attributable to an electrode reaction. This exponential profile of the resistivity is superimposed on a starting value of 1500 Ω·m, corresponding to experimentally obtained values in an acetone/*n*-butylamine medium. It is in fact only in this case as shown in Fig. 4b that our model predicts that the EPD process will be self-limiting i.e., the thickness of the deposit can be controlled by the electric field going to zero at the suspension-deposit interface. Naturally the dry powder itself needs to be a good insulator for this effect to occur and the intrinsic conductivity of the liquid due to ionic species needs to be low.

It should be useful to take advantage of this effect if one is interested in laying down coatings of an insulating substance with a very uniform thickness. This will require work under clean conditions avoiding contamination of the EPD process (e.g., by the powders themselves) and the use of solvents with low ionic concentration.

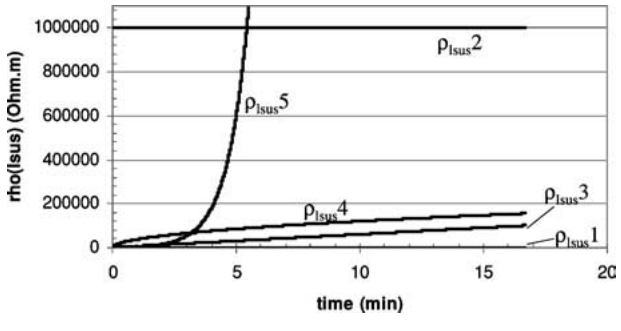


(a)

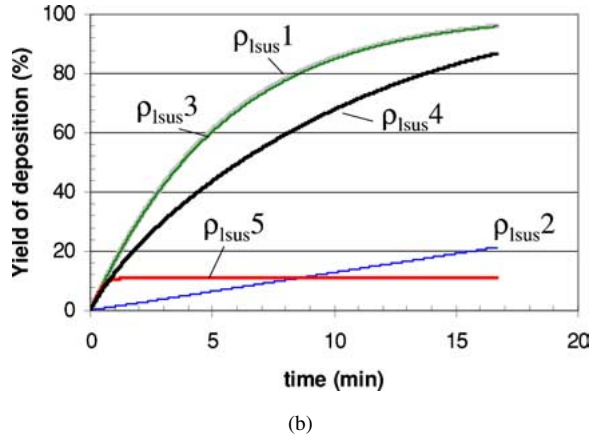


(b)

*Figure 4* (a) Variation of the resistivity of the liquid during EPD used in the calculations of the results in Fig. 4b. $\rho^1_{lsus}$ and $\rho^2_{lsus}$ are constant at respectively 1500 and $10^6$ Ωm·$\rho^3_{lsus}$ $\rho^4_{lsus}$ and $\rho^5_{lsus}$ start at 1500 Ωm and then increase respectively linearly, parabolically and exponentially. (b) Yield as a percentage of the total available powder in the suspension. The specific resistivity of the dry powder $\rho_{pdep}$ is assumed to be constant at $10^{12}$ Ω·m. Different curves show the effect of a specific resistivity for the liquid in suspension, changing during EPD as shown in Fig. 4a.

## 3. Shaping of free standing objects

It has been reported that for traditional ceramics, such as sanitary ware, the main advantage of using electrophoretic deposition is its higher speed, and the low wear of the moulds compared to slip casting [7]. The shaping by EPD of objects with diverse shape has been reported: tiles, coffee mugs, closed and open ended tubes, hemispheres, tubes with changes in diameter and conical shapes are some of the examples made mainly on laboratory scale using solid compositions normally used for table and sanitary ware [3, 8–10]. It is noted that for most cases the shapes can be characterized by a small wall thickness and that full details are often not available.

An example of a hybrid process, somewhere in between tape casting and electrophoretic deposition, is the ELEPHANT process [11]. Continuous tapes of ceramic material are made by depositing on two rolling cylinders, which then press the two slabs together in one long tape. The process was developed for the tile industry. After electrophoretic deposition, the tape is cut, punched, dried and sintered. The economic advantages cited are: lower manpower requirements, low energy consumption, low wear (of moulds) and low maintenance [10]. To the best of our knowledge, the equipment is no longer in use at present.

Technical ceramics such as alumina ($Al_2O_3$) [12–14], silicon carbide (SiC) [15–17] and aluminum nitride (AlN) [18] can also be shaped by electrophoretic deposition. Beta-alumina tubes, used as electrolyte in sodium sulfur batteries, are a classical example of the use of electrophoretic deposition. Whereas charging for many ceramics is related to adsorption or de-sorption of hydrogen ions, the preferential dissolution of sodium ions from the beta-alumina particles during milling, is the main factor leading to their charging [19, 20]. An important advantage that came forward during the investigations regarding these beta-alumina tubes, is that in electrophoretic deposition the difference in density between two or more powders used to produce a material is unimportant, and a homogeneous composition can be ensured. Powers [17] showed this by comparing the composition of the first tube and a seventh tube deposited from a suspension containing a beta-alumina powder with a low soda content (8% $Na_2O$) and one with a higher soda content (14–25%) also containing various additives such as MgO and $Li_2O$.

The shaping capability of the EPD technique should be a consequence of the fact that the deposit follows faithfully the contours of the electrode. This is not

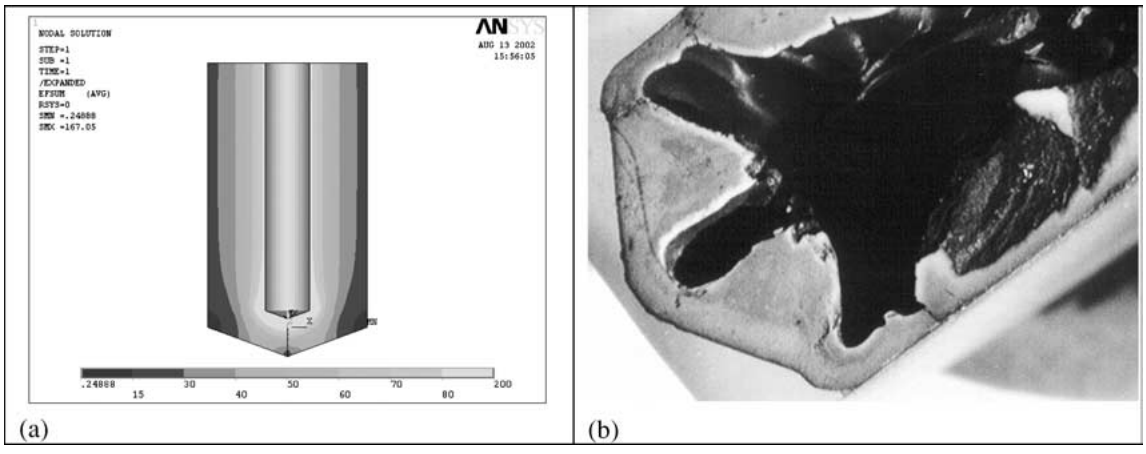


*Figure 5* Electric field calculations between two cylindrical electrodes with conical ends: outer electrode: diameter 18 mm, length 30 mm; inner electrode: diameter 5 mm, length 30 mm (a). Electrophoretically obtained alumina deposit with holes, as predicted from the electric field distribution in (b).

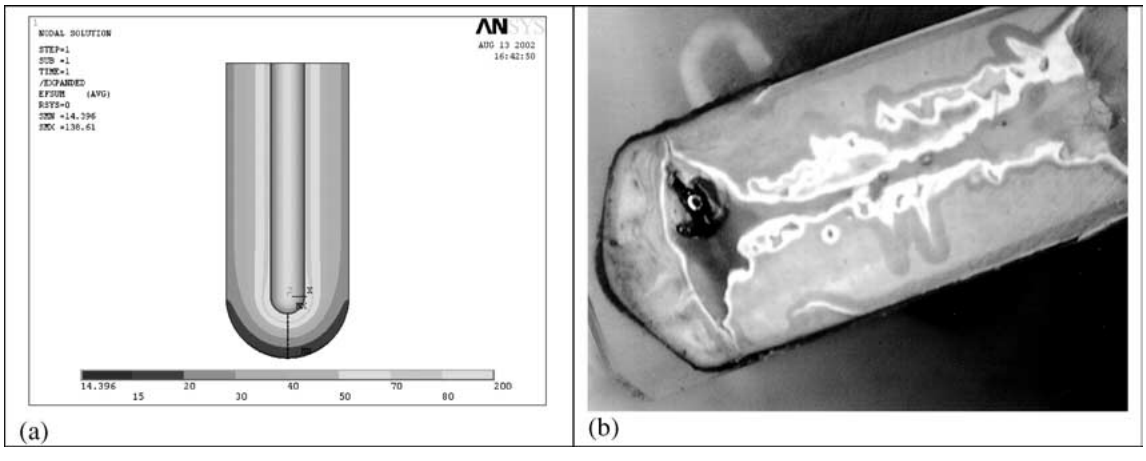


*Figure 6* (a) Electric field distribution between two cylindrical electrodes with spherical end, showing a higher field on the cylindrical wall (diameter counter electrode = 5 mm) and (b) EPD deposit showing faster yield of deposition on cylindrical wall compared to the nearly spherical bottom part.

necessarily so in particular for thicker deposits and free standing objects. Fig. 5, taken from our recent work, illustrates the problem. A cylindrical body needed to be shaped and terminated with a conical surface at one of its ends. The counter electrode was also shaped with surfaces parallel to that of the deposition electrode. During deposition it was noted that cavities in the deposit consistently appeared in the vicinity of the corners of the intended shape, i.e., the top of the cone and the area where the cone and cylinder were joined. In order to explain this, one needs to calculate the electric field distribution. This was done using finite element techniques of the commercially available ANSYS software. The results of these electric field calculations are shown in Fig. 5a. A lower electric field strength is predicted at the corners of the cone. When one compares the result with that of the shape of the deposits, one can readily see that in the areas where the electric field at the deposition electrode is low the deposition rate is consequently also lower. So in accordance with Hamaker's Equation 1, which states that the change in yield of deposition is proportional with the electric field strength one may indeed expect from the electric field calculations the deposition pattern as shown in Fig. 5b.

Of course one has a lot of freedom in the design of the shape of the counter electrode. Indeed it may be possible to design a counter electrode geometry that yields a uniform electric field at a deposition electrode with any reasonably smooth shape. However at present, only intuitive trial and error methods are available to accomplish this. We are not aware of any software that will predict the counter electrode geometry corresponding to a uniform electric field distribution on a deposition electrode with a given shape. Even the combination of a cylindrical shape with a spherical end-cap gives rise to problems. Electric field calculations show that the electric field over the end-cap is now indeed uniform (Fig. 6a), in contrast with the previous case. However, if the radius of the cylindrical part of the counter electrode is the same as that of its spherical end, the field in the cylindrical part is actually higher than in the spherical end cap (this can also be shown by simple analytical expressions). This difference in electric field distribution is again reflected in the deposition rate, which is higher in the cylindrical part than in the approximately spherical part thus leaving a gap between the two sections, as experimentally shown in Fig. 6b.

We have concluded from our experiences to date that the shaping capabilities of the EPD technique for solid free standing forms are constrained by the need to keep the electric field uniform over the deposition electrode. Only rather limited shapes appear possible. Flat shapes

TABLE II EPD parameters in acetone + 10 vol% *n*-butylamine suspension

| | WC-5Co | $Al_2O_3$ | $TiB_2$ | TiC |
|---|---|---|---|---|
| Solids loading (g/l) | 300 | 100 | 100 | 100 |
| Deposition time (s) | 3 | 15 | 3–60 | 3 |
| Critical Deposition time (s) | ±7 | 20 | >? | 10 |
| Applied voltage (V) | 300 | 200 | 300 | 100 |
| Measured Current (mA) | 45–50 | 3–5 | 1–3 | 35–40 |
| Electrophoretic mobility $\mu$ ($m^2$/V·s) | $-8.5 \times 10^{-9}$ | $-10.9 \times 10^{-9}$ | $-13 \times 10^{-9}$ | $-11.6 \times 10^{-9}$ |
| Layer thickness after EPD ($\mu$m) | 125 | 316 | 175–5000 ! | 56 |

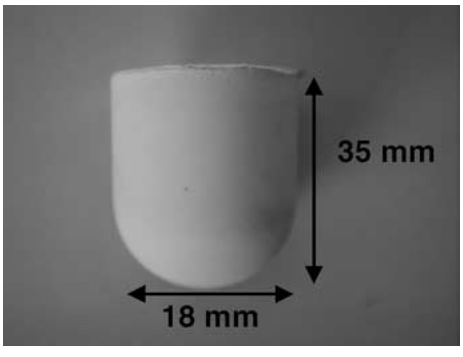


*Figure 7* Cylindrical $ZrO_2/Al_2O_3$ body with hemispherical cap shaped by EPD.

between parallel electrodes, tubes and spheres are possible but deviations from these will give rise to non-uniform wall thickness. In the case presented in Fig. 6 it was possible to produce a cavity free object by adjusting the radii of the cylindrical and spherical counter electrodes. Fig. 7 shows an entirely filled cylindrical body terminated with a hemispherical cap and shaped by EPD.

The shape limitation and electric field problems during EPD is less severe for coatings although we have observed in our work on coatings that local sharp edges which give rise to local electric field enhancement also give rise to a local thickening of an electrically conducting coating.

## 4. Processing of the deposit

Once the required wall thickness has been deposited, the shaped powder needs to be dried and removed from the electrode. Little is known about the structure of the green deposit while still in the suspension. After deposition and drying, high green densities up to 60% have been measured in our work. In general, one needs to take into account that the deposit is saturated with liquid and that some shrinkage has to be accommodated during drying. The shape of the electrode has to allow shrinkage of the deposit. This constraint on possible shapes also occurs in casting technology for instance. For free standing objects, the adhesion between the electrode and the part should be minimum so that they can easily be separated, which is not always readily accomplished. We have often used carbonaceous materials of various kinds. In fact, it has been shown in literature that the formation of a deposit is accompanied by electrode reactions, the products of which not only may strengthen the deposit but also cause adhesion to the electrode. Even when the deposit is easily detached from the electrode without damage, cracks can appear in the drying body due to well-known mechanisms [21]. This problem is increased as the wall thickness of the body is increased.

Cracks due to drying may also limit the maximum thickness of a coating that can be deposited on a dense substrate without carbonaceous interlayers. For instance, we found that the coating thickness of a hard phase on steel bodies was limited due to cracking during drying. Table II summarizes our findings for coatings on cylindrical high speed steel rods with a diameter of 8 mm [22]. It is clear that the thickness below which no cracking is observed depends on the powder.

Surprisingly, we did not find such a critical thickness for a $TiB_2$ powder for which crack-free coatings up to 5 mm thick could be deposited. This suggests that through further improvements of the characteristics of the powder the critical thickness can be increased. Powders with a high critical thickness may also be of interest for forming free standing objects.

## 5. Concluding remarks

EPD appears to be a processing technique which is especially suited for deposition of coatings from particulate suspensions. For electrically insulating powders, one may choose conditions where the growth of the layer is self-limiting by the reduction of the electric field at the deposit-suspension interface. This condition may enhance the uniformity of the thickness of the coating. In any case, further consolidation of the coating is necessary using sintering or curing techniques. EPD can be a rapid coating production technique, much faster than PVD and CVD. Coating thickness is limited and of the order of 100 micrometers, depending on the powder. If a suitable densification technique is applicable, then coatings superior to plasma sprayed coatings should be possible.

Electrophoretic shaping of free standing objects is possible and has been demonstrated in literature and in our own work. The thickness of the deposit and its associated electrical resistance do not pose a fundamental problem during deposition. It is fair to say though that EPD is not widely practiced at the moment for the production of free standing bodies. Flat and smooth thin walled shapes such as tubes and spheres are within easy reach of the technique. In fact the possibility to produce very thin tubular shapes, which are difficult to produce by other techniques such as extrusion and slip casting, may pose an opportunity for the EPD technique.

Other more complicated and thick walled shapes are limited, mainly due to the requirement to secure a uniform electric field along the surface of the deposition electrode. Also separation of objects from the electrode and the avoidance of drying cracks are problems that need a solution, which should not slow down the overall speed of the process. In order to attempt the production of the more complicated shapes, there has to be added value of the EPD technique with respect to other more common processing methods. One such an added value is the enhanced impregnation of fiber preforms [23]. Other examples of added value may be in the production of tough laminated ceramic tubes that fail in a 'graceful' way [24] and the production of functionally graded components with a continuous controlled gradient [25, 26].

## Acknowledgments

This work was supported by the Flemish Institute for the Promotion of Scientific and Technological Research in Industry (IWT) under grant no. SB/993205 and by the Brite-Euram program of the Commission of the European Communities under project contract no. BRPR-CT97-0505.

## References

1. O. VAN DER BIEST and L. VANDEPERRE, *Annual Rev. Mater. Sci.* **29** (1999) 327.
2. J. TABELLION and R. CLASEN, *Key Engin Mater.* **206–213** (2001) 397.
3. H. C. HAMAKER, *Trans. Faraday Soc.* (1940) 279.
4. A. SUSSMAN and T. J. WARD, *RCA Review* **42** (1981) 178.
5. Y. HIRATA, A. NISHIMOTO and Y. ISHIHARA, *Nippon Seramikkusu Kyukai Gakujutsu Ronbinshi* **99** (1991) 108.
6. S. PUT, J. VLEUGELS, G. ANNÉ and O. VAN DER BIEST, *Colloids and Surfaces A: Physicochem. Eng. Aspects* **222** (2003) 223.
7. E. MASSOUD, *Interceram* **2** (1979) 117.
8. M. MIHAILESCU, M. EMANDI, V. VANCEA and M. MARCU., *ibid.* **40**(3) (1991) 165.
9. M. AVELINE, *Industrie Céramique* **581** (1966) 28.
10. M. BONCOEUR and S. CARPENTER, *ibid.* **648** (1972) 79.
11. M. S. CHRONBERG and F. HÄNDLE, *Interceram* **1** (1978) 33.
12. J. M. ANDREWS, J. DRACASS, A. H. COLLINS and D. C. CORNISH, *Proc. Brit. Ceram. Soc.* **12** (1969) 211.
13. R. NAß, H. SCHMIDT, W. STORCH, F. HARBACH, R. NEEFF and H. NIENBURG, in "Ceramic Powder Processing Science", edited by H. Hausner, G. L. Messing and S. Hirano (Deutsche Keramische Gesellschaft, 1989) p. 625.
14. J. H. JEAN, *Mater. Chem. Phys.* **40** (1995) 285.
15. L. VANDEPERRE, O. VAN DER BIEST, F. BOUYER, J. PERSELLO and A. FOISSY, *J. Eur. Ceram. Soc.* **17**(2) (1997) 373.
16. L. J. VANDEPERRE, O. VAN DER BIEST, F. BOUYER and A. FOISSY, *Ceram. Bull.* **77**(1) (1998) 53.
17. H. WITTWER and H. G. KRÜGER, *Ber DKG* **72**(9) (1995) 556.
18. K. MORITZ and T. REETZ, *Ber DKG* **70**(7) (1993) 348.
19. J. H. KENNEDY and A. FOISSY, *J. Electrochem. Soc.* **122**(4) (1975) 482.
20. R. W. POWERS, *Ceram. Bull.* **65**(9) (1986) 1270.
21. G. W. SCHERER, *J. Amer. Ceram. Soc.* **73**(1) (1990) 3.
22. S. PUT, J. VLEUGELS, G. ANNÉ and O. VAN DER BIEST, *J. Mater. Sci.* **39** (2004) 881.
23. A. R. BOCCACCINI and C. B. PONTON, *JOM* (1995) 34.
24. L. VANDEPERRE and O. VAN DER BIEST, *J. Eur. Ceram. Soc.* **18** (1998) 1915.
25. G. ANNÉ, S. PUT, J. VLEUGELS and O. VAN DER BIEST, in Proceedings of the First International Conference on Electrophorectic Deposition: Fundamentals and Applications, August 18–22, 2002, Banff, Alberta, Canada, ISBN 1-56677-345-8, in Proceedings Volume 2002-21 The Electrochemical Society, (2002) p. 206.
26. S. PUT, J. VLEUGELS and O. VAN DER BIEST, *Scrip. Mater* **45**(10) (2001) 1139.

*Received 6 January*
*and accepted 31 January 2003*